NIPAAm-MMA nanoparticle-encapsulated visnagin ameliorates myocardial ischemia/reperfusion injury through the promotion of autophagy and the inhibition of apoptosis

HAIRONG FU[1], XIAOSHAN LI[2] and JIAHUA TAN[3]

Departments of [1]Physiology, [2]Pathology and [3]Physical Education, Chongqing Three Gorges Medical College, Chongqing 404120, P.R. China

Received June 7, 2016; Accepted December 19, 2017

DOI: 10.3892/ol.2018.7922

Abstract. The main method for the treatment of acute myocardial infarction (AMI) is percutaneous coronary intervention; however percutaneous coronary intervention will induce ischemia/reperfusion (IR) injury, resulting in the loss of cardiac function and cardiomyocyte death. An effective drug to target this condition is necessary. N-isopropylacrylamide and methacrylic acid were used to synthesize drug delivery nanoparticles (NP) containing the natural compound visnagin for IR injury treatment. It was demonstrated that NP containing fluorescein isothiocyanate localized to the site of myocardial IR, and that NP-visnagin treatment induced cardioprotection, reducing the size of the MI and ameliorating cardiac dysfunction through the induction of autophagy and the inhibition of apoptosis. In the future, visnagin may be suitable as a drug for IR injury treatment, and NP may be an effective drug delivery system.

Introduction

Acute myocardial infarction (AMI) is a leading cause for mortality worldwide, and coronary heart disease incidence, which may lead to AMI, continues to trend upwards (1). The treatment guidelines for AMI include percutaneous coronary intervention or thrombolytic treatment, which contribute to the early reperfusion of the ischemic region; although these treatments may prevent a certain extent of myocardial damage, an ischemia/reperfusion (IR) injury may occur, resulting in the loss of cardiac function and cardiomyocyte death (2,3). Reducing the extent of IR injury will aid in the improvement of the therapy for AMI.

Correspondence to: Professor Hairong Fu, Department of Physiology, Chongqing Three Gorges Medical College, 366 Tian Xing Road, Bai An Ba, Wan Zhou, Chongqing 404120, P.R. China
E-mail: fuhr_1979@163.com

Key words: acute myocardial infarction, ischemia/reperfusion, N-isopropylacrylamide, methacrylic acid, visnagin

Visnagin, 4-methoxy-7-methyl-5H-furo[3,2-g][1]benzopyran-5-one, is extracted from the fruit of *Ammi visnaga*. Visnagin and related compounds, including khellin and visnadin, are used to treat angina pectoris as they exhibit peripheral and coronary vasodilatation activity (4). Visnagin also can inhibit blood vessel contraction and decrease blood pressure through inhibiting Ca^{2+} channels to prevent calcium influx into the cell (5). It was previously reported that visnagin could prevent oxalate-induced cell death in renal epithelial cells; it also exerted an anti-inflammatory effect on lipopolysaccharide (LPS)-stimulated cells and a neuroprotective effect against kainic acid (KA)-induced neuronal death (6). However, the cardioprotective effect of visnagin for cardiomyocytes in IR injury has not been demonstrated.

In recent years, nanotechnology has been developed and applied in the treatment of various diseases. Nanoparticle-based therapeutic systems, particularly drug delivery systems, have become a popular research field due to their targeting of functional zones to effectively deliver therapies (7). Hydrogels are a drug delivery system based on polymer-controlled release; temperature-sensitive hydrogels are the most commonly researched for drug delivery. N-isopropylacrylamide (NIPAAm) is a temperature-sensitive hydrogel, its lower critical solution temperature (LCST) is 32˚C; when the temperature is below the LCST, it is in a liquid phase, and above the LCST it is in a gel phase (8). To improve the application of hydrogel, co-monomers, including methacrylic acid (MAA), may be used so that hydrogels, including NIPAAm-MAA, also exhibit a pH-responsive characteristic, which is a pH value of ≥6.7 capable of triggering the pH-response (9). The continuous aggregation of NIPAAm-MAA nanoparticles (NP) in the intercellular space of the IR region contributes to the gel formation due to the temperature being higher than that of the LCST, which ensures that the NP can continuously aggregate in the IR region (10). Furthermore, the pH-responsive characteristic of NP guarantees the NP can be solely decomposed in the IR region, due to the pH value of IR region being >6.7, this ensures the NP-encapsulated drugs can be released in the IR region (11,12). Consequently NP may be an optimal drug delivery system for the treatment of IR injury.

Autophagy is a cell-protective process in response to stress. During the process of autophagy, bilayers on the

area of the rough endoplasmic reticulum without ribosomes surround dysfunctional proteins and organelles to form the autophagosome, then fuses with lysosomes to induce the release of lysosomal enzymes, which degrade the contents of the autophagosome, ultimately releasing metabolites for use by the cell (13,14).

In the present study, NIPAAm-MAA nanoparticles (NP) loaded with visnagin were synthesized. Following IR injury, NP were specifically transported to MI, where visnagin was released. The heart function was improved and the infarct size was decreased. Furthermore, light chain (LC) 3II expression and the number of autophagosomes were increased, and apoptosis was inhibited. Therefore, we hypothesize that NP may be the ideal drug delivery system for targeted IR injury treatment, and visnagin may be a novel drug for IR injury treatment.

Materials and methods

Synthesis of NIPAAm-MAA NP. NIPAAm-MAA NP were synthesized in 1,4-dioxane solution through the free radical polymerization of monomers in an N_2 atmosphere. The ratio of NIPAAm to MAA was 8:0.5; they were conjugated with 2-(dimethylamino) ethyl methacrylate (DMAEMA). Benzoyl peroxide (BPO; 0.2 g) was added into the solution to block the reaction; the nanoparticles were obtained at 70˚C for 24 h in an N_2 atmosphere and precipitated.

Scanning electron microscopy (SEM). The size, aggregation and shape of the NP were observed with SEM. SEM was conducted with a high-resolution INSPECT F50 (FEI; Thermo Fisher Scientific, Inc., Waltham, MA, USA). The NP samples were dissolved in water (0.5 mg/ml), heated to 100˚C, then cooled to room temperature. Images of the NP were obtained through SEM.

Drug-loaded NP. The nanoprecipitation method was used to prepare visnagin-loaded NP (NP-visnagin) and fluorescein isothiocyanate (FITC)-loaded NP (NP-FITC). Briefly, 100 mg lyophilized NP was dissolved in 10 ml water and stirred. Visnagin (20 mg) was added into the solution to be directly loaded into the NP. For the FITC loading, 100 mg lyophilized NP were dissolved in 10 ml water and stirred, FITC (10 mg) was then added into this solution. The resultant solution was emulsified in polyvinyl alcohol (0.5 wt%) and chitosan (2 wt%) solution and stirred at 20 x g using a propeller-type agitator with four blades. Following solution agitation for ~1 h, the entire suspension was centrifuged (4,000 x g for 20 min). The supernatant was removed and purified water (5 ml) was added to the sediment. This mixture was centrifuged again to remove the excess polyvinyl alcohol and the unencapsulated reagent. This process was then repeated and the resulting NP-visnagin or NP-FITC was freeze-dried for 24 h and stored at -20˚C until subsequent use.

Drug release assay. The release conditions for NIPAAm-MAA NP were 37˚C and pH 5. NP-visnagin (8.5 mg) was dissolved in 30 ml NaH_2PO_4-Na_2HPO_4 solution at 37˚C. The release of visnagin over time was analyzed through an ultraviolet-visible spectrometer.

Animal model of IR. All animal studies were approved by the ethical committee of Chongqing Three Gorges Medical College (Chongqing, China). A total of 125 male Sprague-Dawley rats (weight 200 g) were purchased from the Experimental Animal Center of Chongqing Three Gorges Medical College (Chongqing, China), and were divided into 8 groups (the sham group comprised of 10 rats; A total of 15 rats were used to perform the optical bioluminescence imaging assay with 3 groups, each group containing 5 rats, and 100 rats were used to perform the agent treatment assays with 4 groups, each group containing 25 rats.). All the rats were fed in a pathogen-free environment, at a temperature between 24-28˚C, ventilated between 10-20 times per hour, with a relative humidity of 50-60%. The light/dark cycle was (natural) circadian light, the food was sterilized by irradiation, and the water contained bacitracin (4 g/l) and neomycin (4 g/l), the food and water were provided adequately. In the experiment process, all the rats were anesthetized with 4% pentobarbital sodium (0.4 ml/100 g) and placed on a 37˚C pad. Rats were ventilated during the procedure with a MiniVent ventilator (Hugo Sachs Elektronik GmbH, March-Hugstetten, Germany). A left thoracotomy was performed to expose the heart, and the left anterior descending coronary artery (LAD) was occluded with a 6-0 prolene suture. The regional ischemia was confirmed through visual inspection. After 45 min ischemia, the ligation was released. Ischemia injury in the tissue was confirmed subsequent to re-perfusion. A sham group of rats underwent the same surgical procedure, without ligation, the results of sham group were used to confirm the successful establishment of IR model (data not shown). All animals were sacrificed under anesthesia at the end of the experiments.

Cardiac function analyses. A total of 30 min after the establishment of the IR model, the rats received PBS (3 ml/kg), NP (5 mg/kg) in saline, visnagin (2 mg/kg) in saline or NP-visnagin (1 mg/kg) in saline, through a caudal vein injection in saline intravenously. Hemodynamic measurements and echocardiography were used to analyze cardiac function in rats. Two weeks after injection, the rats were anesthetized prior to transthoracic M-mode echocardiography using a Vevo770 system (VisualSonics Inc., Toronto, ON, Canada) with a 30-MHz probe (RMV 707B). A total of two weeks following the injection of the reagents, the micromanometer catheter (Millar 1.4F, SPR 835; Millar, Inc., Houston, TX, USA) was used to detect blood pressure by insertion into the right common carotid artery; the Power Laboratory system (ADInstruments, Dunedin, New Zealand) was used to record and analyze blood pressure.

Terminal deoxynucleotidyl transferase dUTP nick end labeling (TUNEL) staining and caspase activity. Apoptosis was detected through TUNEL staining with an *In Situ* Cell Death Detection kit (Roche Diagnostics, Basel, Switzerland) according to the manufacturer's protocol. Total cardiomyocytes were labeled by DAPI, whereas apoptotic cardiomyocytes were labeled with green fluorescein staining. The caspase-3 and caspase-9 activity was detected through a Caspase-3 colorimetric assay kit and a Caspase-9 colorimetric assay kit (BioVision, Inc., Milpitas, CA, USA) according to the manufacturer's protocol, and the caspase activity was detected by a microplate reader at 405 nm.

Infarct size. At 24 h after reperfusion, the LAD was re-occluded and 1% Evans blue dye (Sigma Aldrich; Merck KGaA, Darmstadt, Germany) was injected into the inferior vena cava to identify the area at risk (AAR); the heart was cut into 1 mm-thick cross sections for incubation with 1% 2,3,5-triphenyltetrazolium chloride (TTC, Sigma-Aldrich; Merck KGaA). At 7 days, the left ventricles of the rat hearts were obtained for Masson staining to analyze the infarct site. Photographs were captured with a digital camera (Pentax K-X, Pentax, Inc., Japan). The infarct size was detected with computer-assisted planimetry software (QW in version 3; Leica Microsystems GmbH, Wetzlar, Germany).

Immunofluorescence. LC3 dots and NP-fluorescein isothiocyanate (FITC) were detected with immunofluorescence staining. NP-FITC (2 mg/kg) was injected into the inferior vena cava and hearts were harvested from the mice. All the hearts were immersed in 4% paraformaldehyde for 24 h and then dehydrated in 30% sucrose solutions for 2 h, then dehydrated in ascending ethylic alcohols (50, 70, 80, 90 and 100%) for 15 min at each concentration, cleared with 100% xylene and embedded in 100% paraffin, and following by cutting into 5-μm thick sections. The sections were deparaffinized and hydrated in a graded alcohol series to distilled water, and then were permeabilized with 0.1% triton X-100 for 15 min and washed 3 times with 1% PBS. The sections were incubated with antibodies (Anti-FITC; diltion, 1:500; catalog no. #ab19224; Abcam, Cambridge, UK; LC3, dilution, 1:1,000, CST Biological Reagents Co., Ltd.; catalog no. #3868; and Troponin I; dilution, 1:500; catalog no. #ab10231; Abcam) at 4˚C for overnight. The sections were washed 3 times with 1% PBS, then incubated with the Alexa Fluor® 647-conjucated secondary antibodies [F(ab')2-Goat anti-Mouse IgG (H+L), dilution, 1:500; catalog no. #A-21425 and Donkey anti-Rabbit IgG (H+L), dilution, 1:500; catalog no. #A10043 all Invitrogen; Thermo Fisher Scientific, Inc.] at 37˚C for 2 h. The sections were washed 3 times with 1% PBS and observed through laser scanning confocal microscope at x400 magnification (TCS-SP5; Leica Microsystems GmbH).

Optical bioluminescence imaging (BLI) in vivo. BLI, a reliable noninvasive imaging tool, was used to evaluate the distribution of NP-FITC to the heart. Following the injection of NP-FITC (2 mg/kg) and FITC (1 mg/kg), at 0.5, 1, 6 and 24 h, rats were anesthetized with 4% pentobarbital sodium, placed on the 37˚C pad and imaged with BLI using a Xenogen *in vivo* imaging system (Caliper Life Sciences; PerkinElmer, Inc., Waltham, MA, USA) to detect the fluorescence intensity.

Western blotting. LC3 expression was evaluated by western blot analysis. All the tissue protein was extracted by a Radioimmunoprecipitation assay (Beyotime Institute of Biotechnology, Shanghai, China), and the protein concentration was determined by an Enhanced BCA Protein assay kit (Beyotime Institute of Biotechnology) according to the manufacturer's protocol. A total of 50 μg protein was added per lane and separated by a 12% SDS-PAGE gel, and blotted onto polyvinylidene fluoride (PVDF) membranes. The membranes were blocked in a solution of 5% non-fat dried milk in PBST (0.05% Tween-20 in PBS) for 1 h at room temperature, and incubated with primary antibodies (LC3; dilution, 1:1,000; catalog no. #3868; and GAPDH; dilute on, 1:1,000; catalog no. #5174 both from CST Biological Reagents Co., Ltd., Shanghai, China) overnight at 4˚C. The membranes were washed three times for 10 min in PBST, and incubated with secondary antibody (rabbit IgG, dilution, 1:500; catalog no. #sc-2794; Santa Cruz Biotechnology, Inc., Dallas, TX, USA) at 37˚C for 1 h, and the membranes were washed three times for 10 min in PBST. The immunoreactive signal was detected through the BeyoECL Plus kit (Beyotime Institute of Biotechnology), and the ChemiDocXRS+ (Bio-Rad Laboratories, Inc., Hercules, CA, USA) was used to obtain the images. Image J 3.0 (National Institutes of Health, Bethesda, MD, USA) was used to quantify the band intensity relative to GAPDH.

Transmission electron microscopy (TEM). TEM was used to detect autophagosomes. Following the injection of visnagin-loaded NP, the hearts underwent retrograde perfusion by PBS, and the left ventricle was harvested and fixed with 4% glutaraldehyde for 24 h at room temperature, following post-fixation with 2% osmium tetroxide for 2 h and 1% aqueous uranyl acetate for 1 h at room temperature. The tissue was washed in an ascending series of ethanol (50, 60, 70, 80, 90, 95 and 100%), and transferred to a mixture (10 ml) of propylene oxide and EMbed 812 (Electron Microscopy Sciences, Hatfield, PA, USA; ratio 1:1), the tissue was incubated for 1 h at room temperature, then place in a 60˚C oven to polymerize for 48 h. Sections (80-nm thick) were cut using a Leica ultramicrotome (Leica Microsystems GmbH) and a Diatome diamond knife (Diatome Ltd., Nidau, Switzerland), and were collected on 200-mesh copper grids and stained in 5% uranyl acetate in ethanol for 15 min at room temperature and 5% Reynold's lead citrate for 10 min at room temperature. The slices were then observed with transmission electron microscopy at 40–120 kV (CM10; Philips Medical Systems B.V., Eindhoven, The Netherlands).

Statistical analysis. All the data were expressed as the means ± standard deviation and analyzed by SPSS 17.0 (SPSS, Inc., Chicago, IL, USA). Intergroup comparisons were performed through a t test or analysis of variance followed by Bonferroni post-hoc testing. $P<0.05$ was considered to indicate a statistically significant difference.

Results

Visnagin-loaded NP synthesis. In order to obtain the perfect drug delivery material, NIPAAm and MAA were selected for the synthesis of NP, catalyzed by DMAEMA, BPO and N_2 (Fig. 1A). With the aim of drug delivery, visnagin was loaded into the NP (Fig. 1B); the loading rate was 100% (data not shown). The size and shape of the NP were observed with SEM (Fig. 1C); the size of the NP was approaching 100 nm, and they were microspherical in shape. To determine the release rate for NP-visnagin, a drug release assay was conducted; initially, the release rate linearly increased, indicating that the amount of released visnagin increased over time, whereas the release ratio was decreased from 50 h, and trended towards a halt (Fig. 1D). These results demonstrated that NP synthesized with NIPAAm-MAA were an excellent visnagin-loading

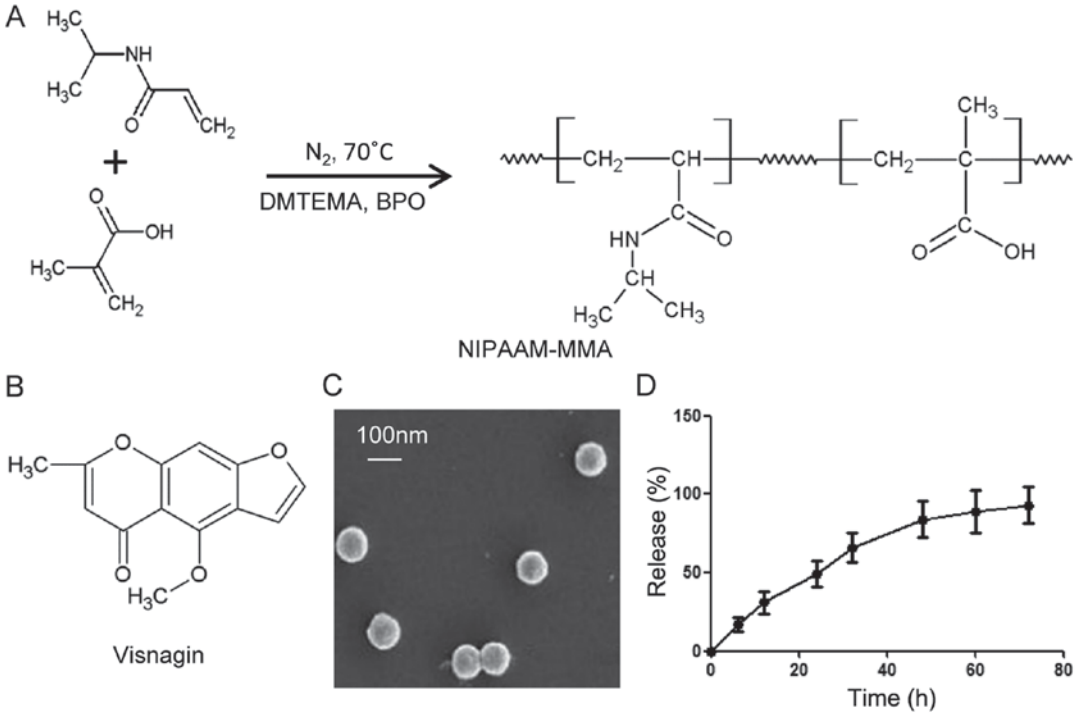

Figure 1. Visnagin-loaded NP synthesis. (A) Synthesis of NP. NIPAAm and MMA were polymerized with DMAEMA and BPO in an N_2 atmosphere at 70˚C. (B) Chemical structure of visnagin. (C) Scanning electron microscopy image of the NP. NP were microspherical in shape and their size was approaching 100 nm. (D) NP-visnagin release curve. NP-visnagin was dissolved in NaH_2PO_4-Na_2HPO_4 solution at 37˚C and at each time point, the sample was analyzed with an ultraviolet-visible spectrometer. NP, nanoparticles; NIPA Am, N-isopropylacrylamide; MAA, methacrylic acid; DMAEMA, 2-(dimethylamino) ethyl methacrylate; BPO, Benzoyl peroxide.

material, and that the characteristics of NP were suitable for visnagin release.

NP-visnagin targeted to the ischemic region to induce cardiomyocyte protection subsequent to IR. To detect the targeting ability of NP, NP-FITC was synthesized for a BLI *in vivo* assay. In the rats with IR injury, at 0.5 h after NP-FITC injection, NP-FITC was concentrated in the heart; the concentration of NP-FITC in the heart increased over time, as demonstrated by the increase in fluorescence (Fig. 2A and B). The PBS-injected group exhibited no fluorescence intensity increase in the heart, and in the group injected with FITC alone, the fluorescence intensity increased to a visibly lesser extent (Fig. 2A and B). Through an immunofluorescence assay, it was indicated that NP-FITC had predominantly localized to the infarcted area after NP-FITC injection (Fig. 2C and D). In addition, treatment with either intravenous NP-visnagin or visnagin alone reduced IR injury at the onset of reperfusion (Fig. 2E and F); based on TTC staining, intravenous NP-visnagin treatment significantly reduced the MI size compared with visnagin alone, and was >2-fold more effective (Fig. 2E and F). Additionally, the percentage AAR in the left ventricle was not significantly different between groups (Fig. 2G). These results demonstrate that NP-visnagin targeted the ischemic region and conferred superior cardioprotection against myocardial IR injury compared with visnagin alone.

NP-visnagin ameliorated cardiac dysfunction at 4 weeks subsequent to IR. Echocardiography results demonstrated that NP-visnagin or visnagin alone significantly ameliorated cardiac dysfunction, although the effect of NP-visnagin was greater (Fig. 3A-C). NP-visnagin significantly decreased the left ventricular end-diastolic dimension and end-systolic dimensions, and increased the left ventricular ejection fraction and fractional shortening (Fig. 3B). Furthermore, NP-visnagin increased the left ventricular systolic pressure and rate of rise of left ventricular pressure (dP/dt), and decreased the left ventricular end-diastolic pressure (Fig. 3C). Thus, NP-visnagin ameliorated cardiac dysfunction through improving the systolic and diastolic function and pressure. Additionally, Masson staining indicated that NP-visnagin significantly inhibited fibrosis (Fig. 3D and E). These results indicated that NP-visnagin or visnagin alone ameliorated cardiac dysfunction and blocked fibrosis, whereas the effect of NP-visnagin was greater.

NP-visnagin enhanced autophagy in the ischemic region after IR. As it had been identified that NP-visnagin protected cardiomyocytes after IR, further study was conducted to reveal the mechanism for the NP-visnagin protection of cardiomyocytes. As autophagy is an established protective mechanism for cells under stress, and LC3 is a marker of autophagic flux, proteins from the AAR were analyzed with a western blot assay. The results demonstrated that NP-visnagin significantly increased the level of LC3II; although visnagin alone also improved the expression of LC3II, the effect of NP-visnagin was greater (Fig. 4A and B). To further confirm NP-visnagin-induced autophagy, immunofluorescence studies were conducted. The results of immunofluorescence were consistent with western blot assay, as both NP-visnagin and visnagin alone could enhance

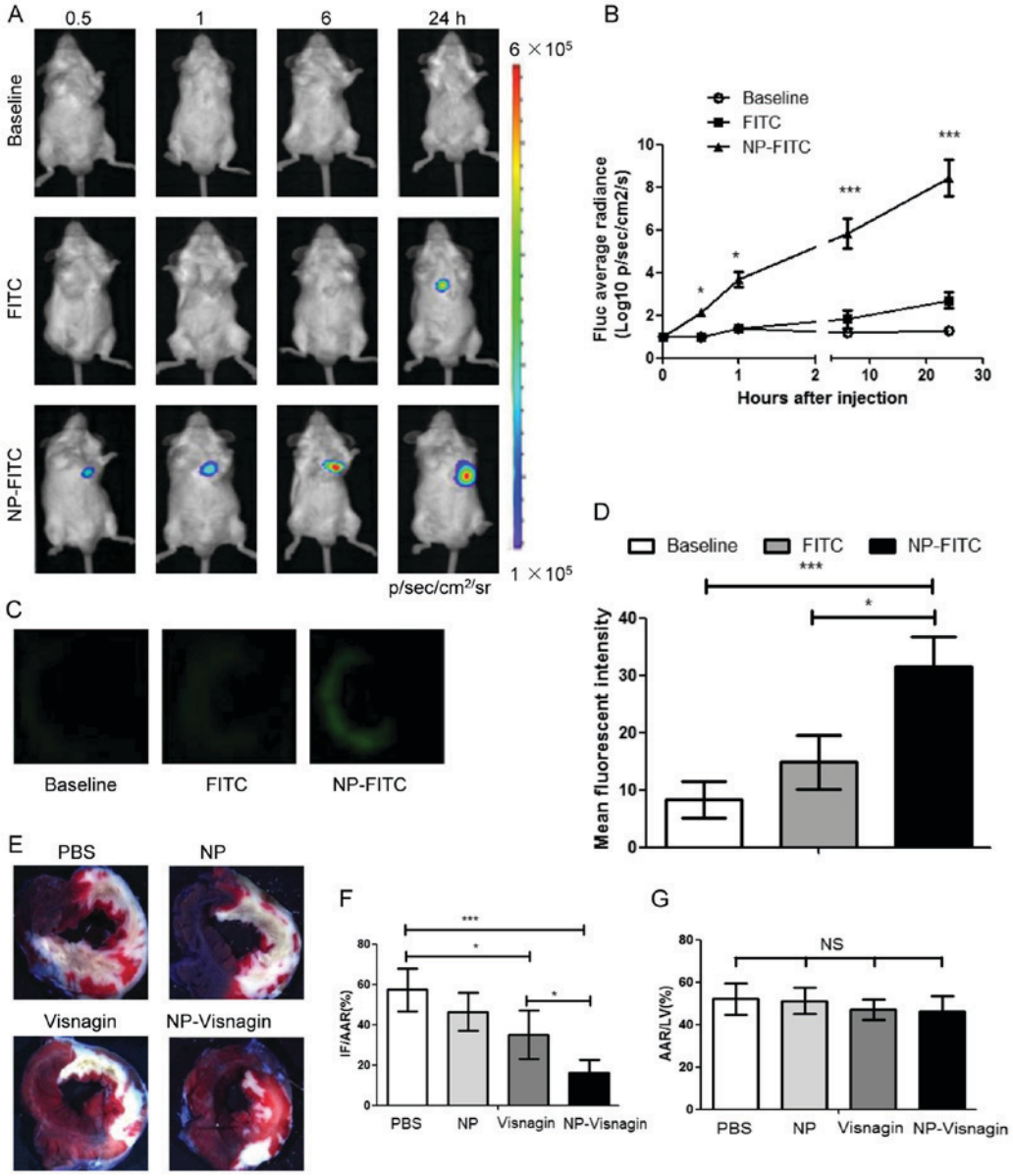

Figure 2. NP-visnagin targeted to the reperfused myocardium and exerted cardioprotective effects. (A) Following the intravenous injection of PBS (baseline), FITC or NP-FITC, *in vivo* BLI was performed at each time point. (B) Quantitative analysis of BLI data for NP-FITC compared with FITC alone. (C) Fluorescence images of heart cross-sections at 12 h after the intravenous injection of PBS, FITC or NP-FITC. (D) Quantification of the fluorescence intensity of the non-ischemic myocardium and AAR. (E) Representative stereomicrographs of heart sections double stained with TTC and Evans blue at 72 h after intravenous injection. (F) Quantitative analysis of IF/AAR. (G) Quantitative analysis of AAR/LV. *P<0.05; ***P<0.005. NP, nanoparticles; FITC, fluorescein isothiocyanate; BLI, bioluminescence imaging; TTC, 2,3,5-triphenyltetrazolium chloride; IF, infarct area; AAR, area at risk; LV, left ventricle; NS, not significant.

the autophagic flux, and the effect of NP-visnagin was greater (Fig. 4C and D). TEM is considered the gold standard for autophagic flux detection; following the NP-visnagin and visnagin treatment of IR injury, the ischemia region was analyzed by TEM. The number of visible bilayer structure bodies was significantly improved following visnagin treatment, with the highest number observed in the NP-visnagin group (Fig. 4E). Collectively, the data demonstrated that NP-visnagin protected cardiomyocytes against IR injury through the induction of autophagy.

NP-visnagin inhibited apoptosis in the ischemic region after IR. In IR injury, apoptosis is the most predominant mechanism for cell death. In order to detect apoptosis, TUNEL and caspase activity assays were used. As demonstrated in Fig. 5A and B, subsequent to IR injury, following treatment PBS or NP treatment, the apoptotic index was significantly increased compared with the effect of visnagin or NP-visnagin treatment, and the effect of NP-visnagin was the most pronounced. Additionally, in the visnagin and NP-visnagin treatment groups, caspase-3 and -9 activity were significantly decreased compared with the PBS and NP groups, and the effect of NP-visnagin was greater (Fig. 5C and D). These results indicated that NP-visnagin inhibited apoptosis in IR injury to protect the damaged cells.

Discussion

In the present study, it was identified that the intravenous injection of NIPAAm-MAA NP specifically targeted the IR

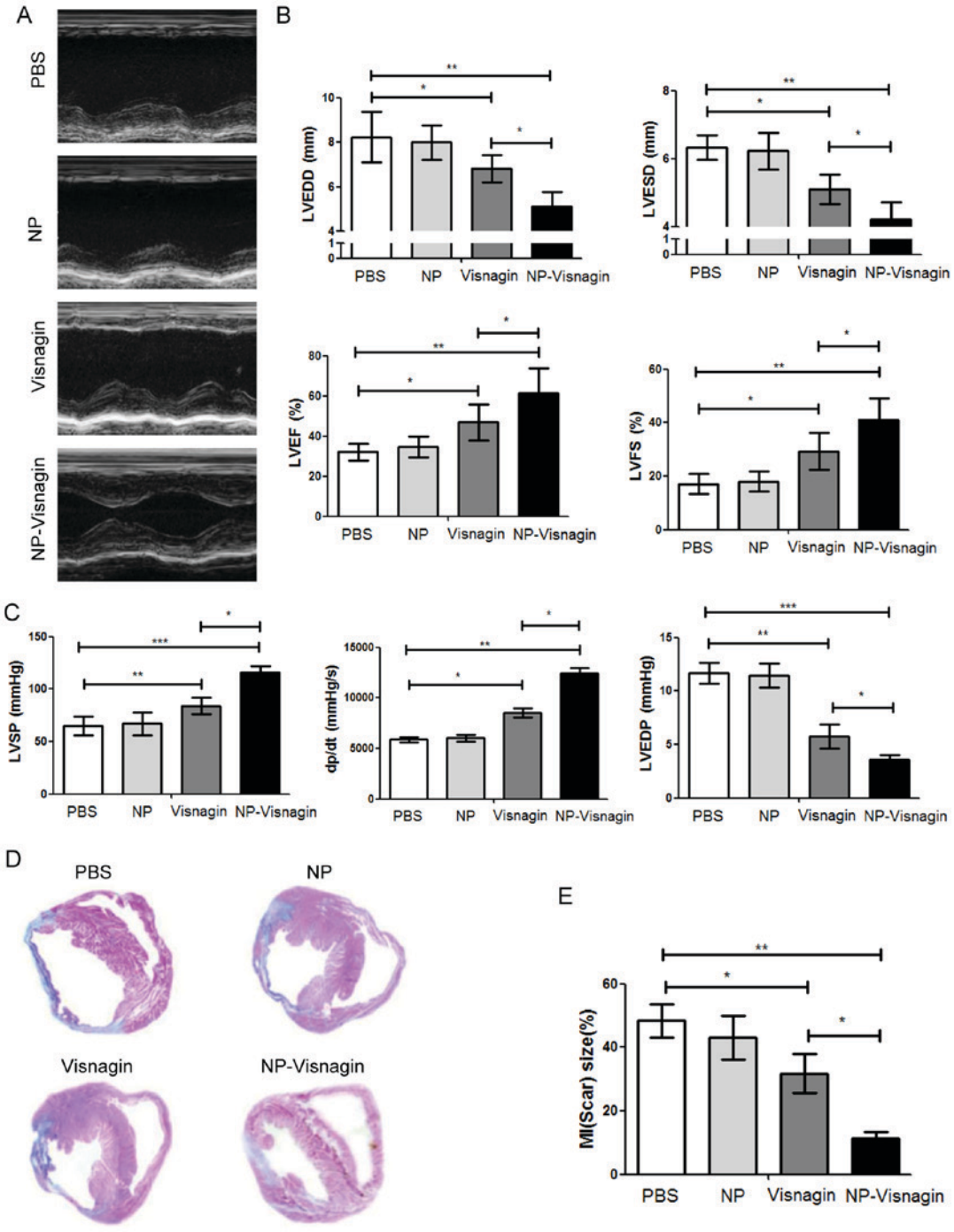

Figure 3. NP-visnagin ameliorated cardiac dysfunction 4 weeks after ischemia/reperfusion. (A) M-mode echocardiography was performed for rats at 4 weeks after intravenous injection with NP-visnagin and other treatments. (B) Effect of NP-visnagin on LVEDD, LVESD, LVEF and LVFS. (C) Systolic blood pressure was detected through the micromanometer catheter method, and the LVSP, the rate of rise of left ventricular pressure (dP/dt) and LVEDP were calculated. (D) Based on Masson staining, the effects of NP-visnagin and the other treatments on fibrosis at 4 weeks after intravenous injection were detected; representative images are shown. (E) Quantification of fibrosis. *P<0.05; **P<0.01; ***P<0.005. NP, nanoparticles; LVEDD, left ventricular end-diastolic dimension; LVESD, left ventricular end-systolic dimension; LVEF, left ventricular ejection fraction; LVFS, left ventricular fractional shortening; LVSP, left ventricular systolic pressure; LVEDP, left ventricular end-diastolic pressure; MI, myocardial infarction.

myocardium after reperfusion; NP-visnagin protected the myocardium against IR injury, reduced the MI region and ameliorated cardiac dysfunction; furthermore, the mechanism for the protective effects of NP-visnagin on the myocardium against IR injury may have included the induction of autophagy and the inhibition of apoptosis.

A previous study demonstrated that patients at a high risk of MI who receive pretreatment with statins prior to ischemia present with a reduced region of MI, whereas treatment with statins had no effect on the MI region when administered at the time of reperfusion (15). In the present study, it was observed that the intravenous injection of NP-visnagin at the time of reperfusion could significantly reduce the MI region at 24 h after reperfusion, as well as ameliorating cardiac dysfunction, and inhibiting fibrosis and hypertrophy at 4 weeks after IR. Although visnagin alone reduced the MI

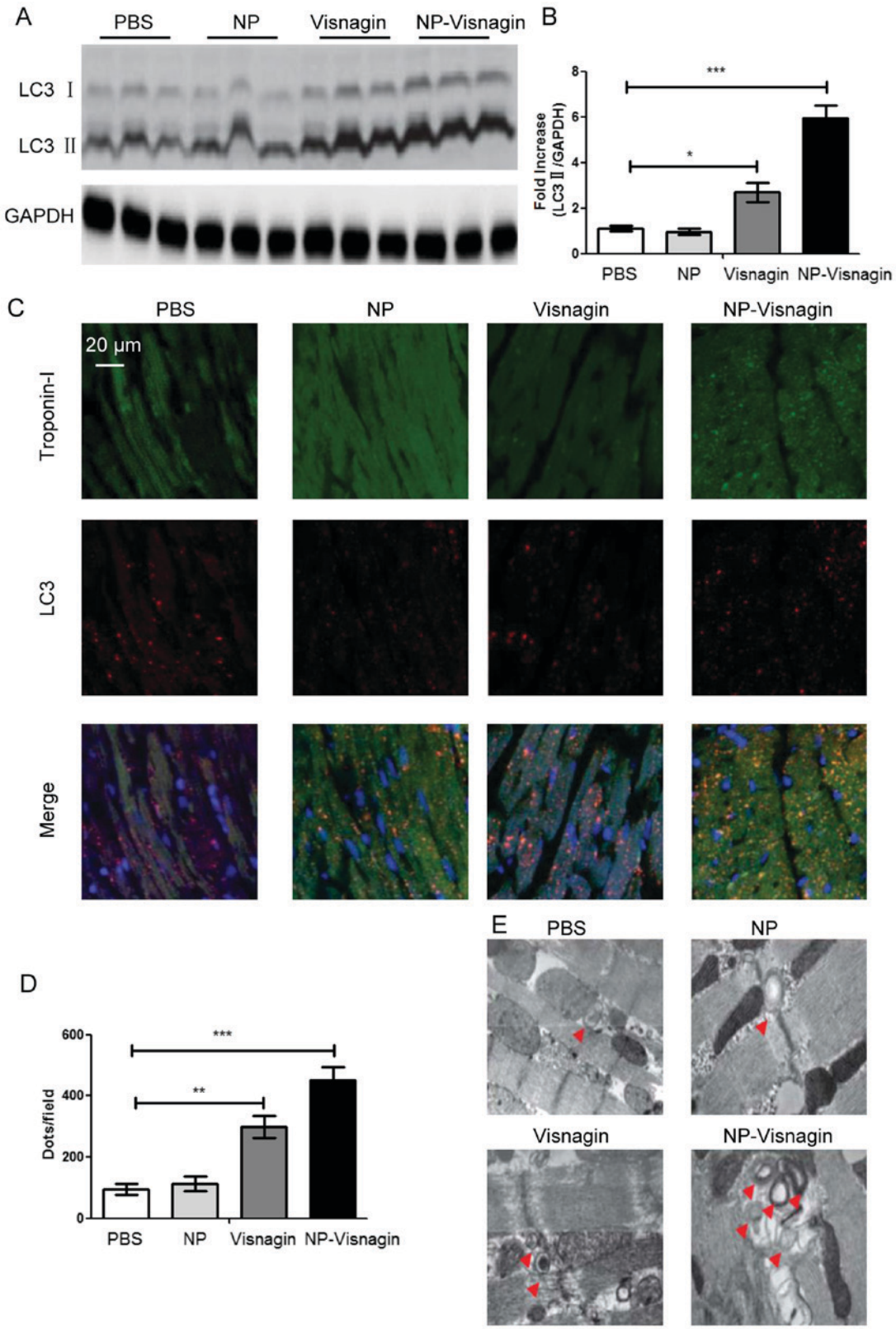

Figure 4. NP-visnagin enhanced the rate of autophagy in the ischemic region after ischemia/reperfusion. (A) Western blotting was performed for the detection of autophagic flux; LC3II was detected in protein harvested from the treated hearts at 24 h after intravenous injection. GAPDH was detected as an internal standard. (B) Quantification of the expression of LC3II relative to GAPDH. (C) Representative images of the immunofluorescence detection of Troponin-I and LC3. Green dyeing represents Troponin-I, indicative of cardiomyocytes, whereas red dots represent autophagosomes. (D) Quantification of LC3 immunofluorescence. (E) Detection of double membrane autophagosomes with transmission electron microscopy. *P<0.05; **P<0.01; ***P<0.005. NP, nanoparticles; LC, light chain.

region and ameliorated cardiac dysfunction, the effect was less than NP-visnagin. These results indicated that visnagin was a potential therapeutic agent for IR injury, and NP could be an ideal delivery material for visnagin. Optical BLI and

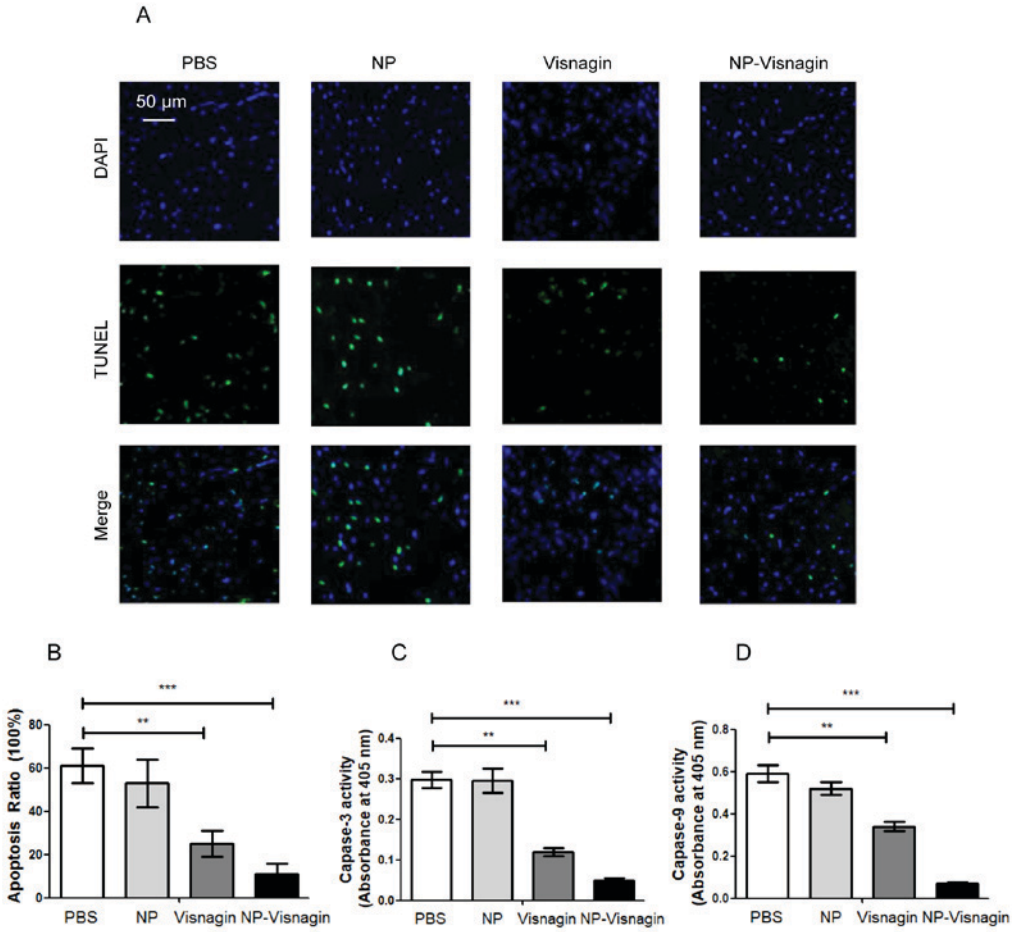

Figure 5. NP-visnagin inhibited apoptosis in the ischemic region subsequent to IR. (A) In order to examine the effect of NP-visnagin on the rate of apoptosis in IR injury, a TUNEL assay was performed; green fluorescence indicates TUNEL-positive nuclei, indicating apoptotic cells, whereas blue fluorescence (DAPI) indicates all cells. (B) Quantification of apoptotic cells. (C) Caspase-3 and. (D) caspase-9 activity of the myocardium subsequent to IR. **P<0.01; ***P<0.005. NP, nanoparticles; IR, ischemia/reperfusion; TUNEL, terminal deoxynucleotidyl transferase dUTP nick end labeling.

fluorescence imaging indicated that intravenously injected NP-FITC was selectively transported into the reperfusion myocardium. Takahama *et al* (16) reported that polyethylene glycol conjugated with liposomes was selectively delivered into the reperfusion myocardium infarct and border region in a rat model, but the precise mechanism by which the liposomes were delivered to the reperfusion myocardium in IR injury was not clarified. The present study identified that NP-FITC was delivered not only to the heart, but also specifically to the infarct site, indicating that NIPAAm-MAA may markedly enhance the drug delivery into the myocardium by improving the vascular permeability. A previous study reported that the reoxygenation of the anoxic cardiac myocardium after IR could induce the uptake of nanoparticles through endocytosis (17).

Visnagin is a natural compound extracted from the fruit of *Ammi visnaga*; it was previously reported that visnagin may exhibit cell protective effects (18). It was demonstrated that visnagin protected kidney epithelial cells against oxalate injury, and neurons against KA-induced apoptosis (19,20). Furthermore, there were reports that visnagin could inhibit LPS-induced inflammation in microglial cells, and that it was a potent cardioprotective compound against doxorubicin-induced cardiomyopathy; a potential mechanism was the binding of mitochondrial malate dehydrogenase by visnagin to trigger the tricarboxylic acid cycle and promote the metabolism of the myocardium (5,21). Additionally, in the field of anti-cancer research, visnagin was also demonstrated to promote aryl hydrocarbon receptor (AHR) signaling, inducing the inhibition of cell growth, differentiation and migration in human hepatocellular carcinoma (22).

Autophagy is a self-protective cell process in response to stress stimulation. It has been reported that autophagy may alleviate metabolic crisis through ATP generation in myocardial IR injury; a low ATP level is an inducer of cardiomyocyte autophagy by the activation of the AMP-activated protein kinase/mammalian target of rapamycin complex 1-Unc-51-like autophagy-activating kinase 1 (ULK1) pathway (23). Cardiac autophagy enables the recovery of energy, and is essential for cardiomyocyte survival. Additionally, autophagy promotes proteostasis in IR injury (13). Once autophagy is activated in IR injury, it can remove cytotoxic ubiquitinated proteins and attenuate protein aggregation. The increase in autophagic activity can compensate for the damage to the ubiquitin proteasome system, and promote the stability of proteolysis. Furthermore, in conditions of reactive oxygen species over-production and inflammatory response in IR injury, the induction of autophagy may remove dysfunctional mitochondria and

recycle waste to maintain the energy balance, preventing damaged mitochondrial from releasing cytotoxic substances, and promoting cardiomyocyte survival (14,24).

In contrast with autophagy, it has been demonstrated that apoptosis may be associated with the pathogenesis of the myocardium in IR injury and contribute to cardiomyocyte death (25). Apoptotic morphological phenotype alterations are observed in IR injury, suggesting that cardiomyocyte apoptosis is stimulated (26). Oxygen free radicals, mitochondrial damage and calcium accumulation are potential inducers of cardiomyocyte apoptosis in IR injury. Oxygen free radicals are generated and accumulated, and ultimately activate a chain reaction leading to the destruction of nucleic acids (27). Mitochondrial damage can contribute to the release of apoptosis-inducing factors from the mitochondria, including apoptotic peptidase-activating factor 1, which can promotes cysteinyl aspartate-specific proteases (i.e. caspases) to induce apoptosis. The accumulation of Ca^{2+} in the mitochondria may activate mitochondrial membrane permeability transition pores and contribute to the release of cytochrome c into the cytoplasm, which activates caspases to induce apoptosis (28).

Previous studies have demonstrated that AHR signaling participates in the modulation of autophagy and apoptosis. AHR is upstream of the Beclin1/Bcl2 complex; it can inhibit the interaction between Beclin1 and Bcl2 to contribute to the release of Beclin1. However, AHR may also promote the development of the autophagy-related 14 (Atg14)-Vps34 complex into the Atg14-Vps34-ULK1 complex, which acts as an activator of autophagy (29-31). AHR is also the activator of anti-apoptotic proteins, including Bcl2, Bcl-XL and survivin, and the inhibitor of pro-apoptotic proteins, including Bcl2-associated X, Bcl2-interacting protein and P53 (32,33). Visnagin has been reported as an inducer of AHR (20,22); it was identified in the present study that NP-visnagin could significantly promote autophagy and inhibit apoptosis in the ischemia region. This indicated that the protective mechanism of NP-visnagin may be through the induction of autophagy and the inhibition of apoptosis.

In summary, it was demonstrated that NIPAAm-MAA NP loaded with visnagin targeted the IR myocardium with cardioprotective effects, reducing the MI size and ameliorating cardiac dysfunction through the induction of autophagy and the inhibition of apoptosis. NIPAAm-MAA NP-based technology may be useful as a novel drug delivery system for IR injury treatment. Additionally, the identification of the cardioprotective effects of visnagin suggests that visnagin may be a novel potential drug for IR injury treatment, although its cardioprotective mechanism requires further clarification.

Acknowledgements

The present study was supported by Chongqing Municipal Education Commission Science and Technology Research Projects (grant no. KJ1502605).

Competing interests

The authors declare that they have no competing interests.

References

1. Capodanno D: Long-term EXAMINATION of drug-eluting stents in acute myocardial infarction. Lancet 387: 316-318, 2016
2. Doll JA and Roe MT: Time to treatment as a quality metric for acute STEMI care. Lancet 385: 1056-1057, 2015.
3. Inoue T: Ischemia-reperfusion injury is still a big hurdle to overcome for treatment of acute myocardial infarction. J Cardiol 67: 305-306, 2016.
4. Kaul B and Staba EJ: Visnagin: Biosynthesis and isolation from ammi visnagi suspension cultures. Science 150: 1731-1732, 1995.
5. Liu Y, Asnani A, Zou L, Bentley VL, Yu M, Wang Y, Dellaire G, Sarkar KS, Dai M Chen HH, *et al*: Visnagin protects against doxorubicin-induced cardiomyopathy through modulation of mitochondrial malate dehydrogenase. Sci Transl Med 6: 266ra170, 2014.
6. Abu-Hashem AA and El-Shazly M: Synthesis, reactions and biological activities of furochromones: A review. Eur J Med Chem 90: 633-665, 2015.
7. Hu CM, Fang RH, Luk BT and Zhang L: Nanoparticle-detained toxins for safe and effective vaccination. Nat Nanotechnol 8: 933-938, 2013.
8. Bearat HH, Lee BH and Vernon BL: Comparison of properties between NIPAAm-based simultaneously physically and chemically gelling polymer systems for use in vivo. Acta Biomater 8: 3629-3642, 2012.
9. Chao TI, Xiang S, Lipstate JF, Wang C and Lu J: Poly(methacrylic acid)-grafted carbon nanotube scaffolds enhance differentiation of hESCs into neuronal cells. Adv Mater 22: 3542-3547, 2010.
10. Zeighamian V, Darabi M, Akbarzadeh A, Rahmati-Yamchi M, Zarghami N, Badrzadeh F, Salehi R, Mirakabad FS and Taheri-Anganeh M: PNIPAAm-MAA nanoparticles as delivery vehicles for curcumin against MCF-7 breast cancer cells. Artif Cells Nanomed Biotechnol 44: 735-742, 2016.
11. Kim SW, Oh KT, Youn YS and Lee ES: Hyaluronated nanoparticles with pH- and enzyme-responsive drug release properties. Colloids Surf B Biointerfaces 116: 359-64, 2014.
12. Boateng S and Sanborn T: Acute myocardial infarction. Dis Mon 59: 83-96, 2013.
13. Sala-Mercado JA, Wider J, Undyala VV, Jahania S, Yoo W, Mentzer RM Jr, Gottlieb RA and Przyklenk K: Profound cardioprotection with chloramphenicol succinate in the swine model of myocardial ischemia-reperfusion injury. Circulation 122: S179-S184, 2010.
14. Przyklenk K, Undyala VV, Wider J, Sala-Mercado JA, Gottlieb RA and Mentzer RM Jr: Acute induction of autophagy as a novel strategy for cardioprotection: Getting to the heart of the matter. Autophagy 7: 432-433, 2011.
15. Hirsch A, Windhausen F, Tijssen JG, Verheugt FW, Cornel JH and de Winter RJ: Long-term outcome after an early invasive versus selective invasive treatment strategy in patients with non-ST-elevation acute coronary syndrome and elevated cardiac troponin T (the ICTUS trial): A follow-up study. Lancet 369: 827-835, 2007.
16. Takahama H, Minamino T, Asanuma H, Fujita M, Asai T, Wakeno M, Sasaki H, Kikuchi H, Hashimoto K Oku N, *et al*: Prolonged targeting of ischemic/reperfused myocardium by liposomal adenosine augments cardioprotection in rats. J Am Coll Cardiol 53: 709-717, 2009.
17. Cabigas EB, Ding G, Chen T, Saafir TB, Pendergrass KD, Wagner MB and Davis ME: Age- and chamber-specific differences in oxidative stress after ischemic injury. Pediatr Cardiol 33: 322-331, 2012.
18. Ragab FA, Hassan GS, Yossef HA and Hashem HA: Synthesis of 6- and 9-alkylaminomethyl furoflavones as gastroprotective agents. Eur J Med Chem 42: 1117-1127, 2007.
19. Badr JM, Hadad GM, Nahriry K and Hassanean HA: Validated HPLC method for simultaneous estimation of khellol glucoside, khellin and visnagin in Ammi visnaga L. fruits and pharmaceutical preparations. Nat Prod Res 29: 593-601, 2015.
20. Kwon MS, Lee JK, Park SH, Sim YB, Jung JS, Won MH, Kim SM and Suh HW: Neuroprotective Effect of Visnagin on Kainic Acid-induced Neuronal Cell Death in the Mice Hippocampus. Korean J Physiol Pharmacol 14: 257-263, 2010.
21. Lee JK, Jung JS, Park SH, Park SH, Sim YB, Kim SM, Ha TS and Suh HW: Anti-inflammatory effect of visnagin in lipopolysaccharide-stimulated BV-2 microglial cells. Arch Pharm Res 33: 1843-1850, 2010.

22. Vrzal R, Frauenstein K, Proksch P, Abel J, Dvorak Z and Haarmann-Stemmann T: Khellin and visnagin differentially modulate AHR signaling and downstream CYP1A activity in human liver cells. PLoS One 8: e74917, 2013.
23. Gatica D, Chiong M, Lavandero S and Klionsky DJ: Molecular mechanisms of autophagy in the cardiovascular system. Circ Res 116: 456-467, 2015.
24. Dutta D, Calvani R, Bernabei R, Leeuwenburgh C and Marzetti E: Contribution of impaired mitochondrial autophagy to cardiac aging: Mechanisms and therapeutic opportunities. Circ Res 110: 1125-1138, 2012.
25. Kolwicz SC Jr, Purohit S and Tian R: Cardiac metabolism and its interactions with contraction, growth, and survival of cardiomyocytes. Circ Res 113: 603-616, 2013.
26. Nishida K, Yamaguchi O and Otsu K: Crosstalk between autophagy and apoptosis in heart disease. Circ Res 103: 343-351, 2008.
27. Kolwicz SC Jr, Purohit S and Tian R: Cardiac metabolism and its interactions with contraction, growth, and survival of cardiomyocytes. Circ Res 113: 603-616, 2013.
28. Viola HM, Arthur PG and Hool LC: Transient exposure to hydrogen peroxide causes an increase in mitochondria-derived superoxide as a result of sustained alteration in L-type Ca2+ channel function in the absence of apoptosis in ventricular myocytes. Circ Res 100: 1036-1044, 2007.
29. Zhang Y, Dong S, Wang H, Tao S and Kiyama R: Biological impact of environmental polycyclic aromatic hydrocarbons (ePAHs) as endocrine disruptors. Environ Pollut 213: 809-824, 2016.
30. Ni HM, Bhakta A, Wang S, Li Z, Manley S, Huang H, Copple B and Ding WX: Role of hypoxia inducing factor-1β in alcohol-induced autophagy, steatosis and liver injury in mice. PLoS One 9: e115849, 2014.
31. Farrall AL and Whitelaw ML: The HIF1alpha-inducible pro-cell death gene BNIP3 is a novel target of SIM2s repression through cross-talk on the hypoxia response element. Oncogene 28: 3671-3680, 2009.
32. Vilahur G , Cubedo J, Casani L, Padro T, Sabate-Tenas M, Badimon JJ and Badimon L: Reperfusion-triggered stress protein response in the myocardium is blocked by post-conditioning. Systems biology pathway analysis highlights the key role of the canonical aryl-hydrocarbon receptor pathway. Eur Heart J 34: 2082-2093, 2013.
33. Qi Y, Tian X, Liu J, Han Y, Graham AM, Simon MC, Penninger JM, Carmeliet P and Li S: Bnip3 and AIF cooperate to induce apoptosis and cavitation during epithelial morphogenesis. J Cell Biol 198: 103-114, 2012.